Rock Type Classification by Multi-band TIR of ASTER

Hiroshi Watanabe
Earth Remote Sensing Data Analysis Center
Forefront Tower, 3-12-1 Kachidoki, Chuo-ku, Tokyo 104-0054, Japan
watanabe@ersdac.or.jp

Kazuaki Matsuo
MC Exploration Co., Ltd
Fukukawa Building 5F, 2-6-1 Marunouchi, Chiyoda-ku, Tokyo 100-0005, Japan
Kazuaki.Matsuo@shell.com

Abstract: The ASTER TIR (thermal infrared radiometer) sensor has 5 spectral bands over 8 to 12 μm region. Rock type classification using the ASTER TIR nighttime data was performed in the Erta Ale range of the Ethiopian Rift Valley. Erta Ale range is the most important axial volcanic chain of the Afar region. The petrographic diversity of lava erupted in this area is very important, ranging from magnesian transitional basalt to rhyolites.
We tried to classify the rock types based on the spectral behavior of each volcanic rock types in thermal infrared range and estimated SiO_2 content with emission data by the ASTER TIR.
Keywords: ASTER, TIR, Erta Ale range, rock type classification, SiO_2 content

1. Introduction

The Erta Ale range is the main volcanic unit in the Afar (or Danakil) depression. It is located along the axis of the northern part of the Afar Triangle of Ethiopia in a zone clearly related to the Red Sea Rift. The extension direction of the main Ethiopian rift is NW-SE and the direction has been rotated clockwise for about 20 degree in the time interval 2.83 to 0.023 Ma by interpreting high resolution images obtained from Landsat TM and SPOT satellites (Korme, Chorowicz, Collet and Banavia, 1997).

The petrographic diversity of lava erupted in this area is very important, ranging from magnesian transitional basalt to rhyolites. There are six principal volcanic centers in the range from north to south, Gada Ale, Alu Dala Filla, Borale Ale, Erta Ale, Hyli Gub and Ale Gub. These volcanoes are all at a stage of fumarolic activity, some of them quite strong indeed, with the exception of Erta Ale in the craters of which molten lava lakes are usually present. Cumulatively erupted mass (relative to December 1968) which combined relative radiation, sensible heat fluxes and lava lake levels (relative to the rim of the central pit) obtained from Landsat MSS, Landsat TM, JERS-1 OPS and ADEOS AVNIR satellites imagery (Oppenheimer, Francis, 1997).

A new optical sensor ASTER is mounted on the TERRA satellite that was launched on December 18, 1999. The ASTER is an advanced optical sensor comprised of 14 spectral channels ranging from the visible to thermal infrared region. It will provide scientific and also practical data regarding various fields related to the study of the earth. The ASTER TIR (thermal infrared radiometer) is an advanced spaceborne radiometer with five spectral bands in the thermal infrared region (8.0-12.0 μm). Its ability to measure thermal emission properties will be useful for locating mineral resources, characterizing the land and sea surface, and observing the atmosphere. Accordingly, we applied the ASTER TIR to the rock type classification in the Erta Ale range, Ethiopia and discussed the effectiveness of the TIR multi-spectral range. The Erta Ale range is the main volcanic chain of the Afar depression. This area is the one of the key regions for the geology of East Africa, located as it is, at the intersection of three of the main structural units affecting the earth crust in that zone, *i.e.* Red Sea, The Gulf of Aden and East African Rift. In spite of its geological importance, Afar has been neglected for a long time by geologists, mainly because of its difficulty to access. The complete geological ground truth started from 1970's (Barberi and Varet, 1970). They brought us a lot of important geological evidences.

Thermal infrared region (8.0-14.0 μm) is affected by the thermal emission from land surface. Consequently, the emission spectrum is one of the important factor for the thermal infrared region in the remote sensing of the earth observation. The emission spectrum in the thermal infrared region is applied to various areas as the useful data in the process of a scientific approach, *i.e.* mineralogy, volcanology and meteorology. Basically, the emission spectrum represents the signature caused by the vibration process between the molecules. The spectral patterns of the rock forming minerals (silicate minerals) show the most characteristic behavior in the thermal infrared region. Consequently, the understanding of the individual spectral behavior is

important to the geological and mineralogical analysis. Clay and carbonate minerals show a characteristic spectral behavior in short wave infrared region (1.3-3.0 μm) and also in the thermal infrared region. Therefore, its usefulness to determine the mineral type identification in mining (clay types, alternated zone in metal deposits, etc.) is well-known and reported in a number of past studies. Most important minerals to be determined by the thermal infrared spectral region are the silicate minerals, which are distinguished into six types of crystal structures based on the SiO_4 tetrahedral chain. The spectral patterns are changed with the SiO_4 tetrahedral structure and chemical compositions. The maximum value of the emissivity named for "Christiansen Peak" in 7.0 to 9.0μm of thermal infrared range shifts from 7.0μm region (silicic rocks) to 9.0μm region (mafic rocks) in concordance with the decrease of SiO_2 content. Moreover, the absorption spectral patterns due to Si-O bond vibration appear in 8.5 to 12.0μm in wavelength region. Minimum value of emissivity is recognized around 9.0μm for tectosilicates. Its position shifted to longer wavelength region up to around 11.5μm for solosilicates and nesosilicates affected by less bond force of the SiO_4 tetrahedral structure.

2. Geological Setting

The northern Afar is a well-defined depression, bounded by the Ethiopian Escarpment on the west and the Danakil Horst on the east. The depression is mainly filled with recent sediments, evaporite beds and covered by extensive lava flows. The sedimentation started in the early Miocene with the detrital series, and continued in the Quarternary by piedmont continental sediments and marine carbonates. This region became arid after its isolation from the Red Sea and a very thick evaporite formation was formed in its central part as "Salt Plain" (Fig. 1).

The Afar depression is one of the key region for the geology of East Africa, located at the intersection of three of the main structural units, which are the Red Sea, the Gulf of Aden and the East African Rift. The region is characterized by intense tectonic and volcanic activities. The main tectonic features are vertical step faulting and open fissures. Fault throws reach 200m. A series of NNW-SSE and N-S faults affect the Ethiopian plateau in the proximity of the step scarp bordering the depression. It is in fact characterized by the presence of a unique trend of the Eritrean or the Red Sea (NNW-SSE direction). The volcanic activity is important since the Miocene. It is today mostly confined to the axial zone, forming three spectacular volcanic chains ; the Erta Ale, the Alayta and Tat Ali.

The Erta Ale chain (about 80km long) is located in the south of the Salt Plain, and is composed of seven volcanic centers, roughly NNW-SSE aligned : Gada Ale, Alu Dala Filla, Borale Ale, Erta Ale (famous for its lava lake), Ale Bagu and Hayli Gub, from north to south. A great diversity of lava compositions ranging from magnesian basalts to rhyolites has been reported in the previous studies (Barberi and Varet, 1970, Barrat, Fourcade, Jahn, Cheminee and Capdevila, 1998, Pik, Deniel, Coulon, Yirgu, Hofmann and Ayalew, 1998).

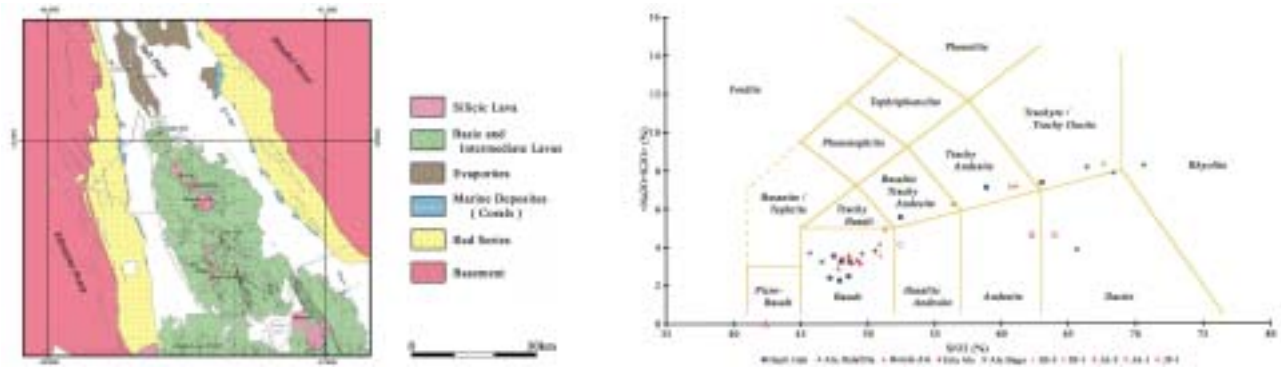

Fig. 1. A geological map <*left*> of the Erta Ale range In the Afar depression, Ethiopia (modified after F. Barberi and J. Varet, 1970) and total alkaline and silica diagram <*right*> for the volcanic rock series of the Erta Ale range. JB-3 to JP-1 are standard volcanic rock samples in Japan. Major element data were referred to the study by J. A. Barrat, 1998 and Geological Survey of Japan, 1994.

3. Characteristics of ASTER TIR

3.1 TIR Functional Parameters

ASTER is an advanced optical sensor comprised of 14 spectral channels ranging from the visible to thermal infrared region. It provides scientific and also practical data regarding various fields related to the study of the earth. ASTER TIR (thermal infrared radiometer) is the first advanced spaceborne multi-spectral radiometer with five spectral bands in the thermal infrared (8-12 μm). Its ability to measure thermal emission properties will be useful for locating mineral resources, characterizing the land and sea surface, and observing the atmosphere. Functional parameters of ASTER TIR are summarized in Table 1.

3.2 Available ASTER TIR Data for the Erta Ale Range of the Ethiopian Rift

The Erta Ale Range is located at near north border of Ethiopia. First image of the Erta Ale Range by ASTER TIR was acquired in the nighttime of February 26, 2000, which was just in the engineering initial check-out period for the ASTER instruments. Data processing level was level 0 (L0B1; data of no geometric and radiometric corrections) at that time, but we tried to make false color composite image and decorrelation stretched image (Fig. 2). We were satisfied with data quality and normal operation of the ASTER TIR.

The complete operation of ASTER GDS (Ground Data System) and the data distribution for researchers started from December 1, 2000. Five data sets of the ASTER TIR covering the Erta Ale range have been processed to level 1B by June 2001 (Table 2). Decorrelation stretched composite images for the nighttime data are shown in Fig. 3. It is able to judge that the ASTER TIR keeps stable on the data quality.

Table 1. ASTER TIR function parameters.

Spectral Bands	Band 10 : 8.125 - 8.475 μm Band 11 : 8.475 - 8.825 μm Band 12 : 8.925 - 9.275 μm Band 13 : 10.25 - 10.95 μm Band 14 : 10.95 - 11.65 μm
Radiometric Resolution	NEδT : 0.3 K
Geometric Resolution	90 m
Pointing Coverage	± 8.55 deg
IFOV	127.8 μ rad
Detector	50 effements (HgCdTe)
Quantization Bit Number	12 bits
Scan Period	4.398 msec
MTF	> 0.25 (cross-track) > 0.20 (along-track)
Scanning Method	Mechanical Scanning (Oscillating Mirror)
Cooler	Linear Drive Stirling Cycle Crycooler

Table 2. Available data set of ASTER TIR for the Erta Ale Range of the Ethiopian Rift.

Scene ID	Acquisition Date	Scene Center	
ASTL1B T (ASTL1A0012041954300012140665)	2000 / Dec. / 04	N12.25	E40.53
ASTL1B T (ASTL1A0012041954390012140666)	2000 / Dec. / 04	N12.57	E40.46
ASTL1B T (ASTL1A00122919484601011210 48)	2000 / Dec. / 29	N13.16	E40.47
ASTL1B T (ASTL1A00122919485501011210 49)	2000 / Dec. / 29	N13.48	E40.40
ASTL1B T (ASTL1A0101301948110102060573)	2001 / Jan. / 30	N13.16	E40.47
ASTL1B T (ASTL1A0101301948200102060574)	2001 / Jan. / 30	N13.48	E40.40
ASTL1B T (ASTL1A0102151948000102230126)	2001 / Feb. / 15	N13.16	E40.45
ASTL1B T (ASTL1A0102151948090102230127)	2001 / Feb. / 15	N13.48	E40.37
ASTL1B T (ASTL1A0006280811400012270775)	2000 / Jun. / 28	N13.55	E40.19

4. Thermal Emission Spectrum of Volcanic Rocks

In thermal infrared region, the thermal emission from the land surface is superior to the reflectance. Most important minerals to be determined by the thermal infrared spectral region are the silicate minerals. The petrographic diversity of volcanic rocks in the Erta Ale Range have bimodal composition ranging from basalt to rhyolite in the median zone between tholeiite and alkalic rock group (Fig. 1). The typical emissivity curves for each volcanic rocks and massive quartz samples which were collected in Japan (these are selected as equivalent to rock types in Erta Ale Range) are shown in Fig. 4.

The emissivity curve of massive quartz indicates clear absorption at band 10, band 12 and indicates clear reflection spike at band 11 on the contrary. In band 13 and band 14 spectral range, it is changing to higher emissivity value. If SiO_2 content in the rock increases, the emissivity curve is expected to indicate a pattern similar to massive quartz. If we classify the rock type whether mafic or silicic on the image, it should be better to select the band combinations 10, 12 and 13 or 14 in blue, green and red respectively (B:G:R=10:12:13 or 14) to make a false color composite image. If the SiO_2 content increases in the rock, the area will appear reddish hue.

On the other hand, right hand side of Fig. 4 represents the reflectance curves for each silicate mineral group in thermal infrared range. The peak of reflectance curve shifts gradually to longer wavelength region from tectosilicate to nesosilicate mineral groups evidently. As a result of this, the maximum absorption peaks of the emissivity curves for each type of silicate group will be expected to shift as same as behavior of the reflectance curves. The ASTER TIR range covers the individual spectral pattern for each silicate type in its range. Accordingly, the ASTER TIR is expected to be a useful tool to classify the rock types based on silicate minerals.

Tectosilicate minerals are represented by quartz and feldspar group. Generally, almost of silicic rocks include the quartz phenocrysts. Fig. 5 (left) is showing the reflectance curves for coarse and fine quartz. The difference between each reflectance curve can be recognized at the band 13 and 14 ranges, which is a point to show a broad peak on spectral curve for fine quartz. In the false color image of B:G:R=10:12:14 in a region occupied by silicic rocks, the rock type with coarse quartz phenocryst tend to appear more reddish hue than the rocks rich in fine quartz phenocryst. On the other hand, the rock type with fine quartz phenocryst or microphenocryst will appear more whitish hue. Fig. 5 (center) shows the reflectance curves for the main type of feldspar group. The feldspar group is divided into three types based on potassium, calcium and sodium components. They are named for orthoclase (K-feldspar), anorthite (Ca-feldspar) and albite (Na-feldspar) in geology. Orthoclase is typically included in the plutonic rocks such as granite and pegmatite etc. Its spectral curve shows highest reflectance in feldspar group. A noticeable difference is recognized on the reflectance strength in each type of feldspar, but the absorptive behavior is good for at any of band 12 range. In the false color image of B:G:R=10:12:14 in a region occupied by igneous rocks, if abundant feldspar is included in the rock, its color shade on the image should be appeared in bluish to magenta hue. In addition to this expectation, a rock type abundant in Ca-rich feldspar such as anorthite appears more bright hue on the image than K-rich feldspar. If Na-rich feldspar is recognized in the rock, the color shade should be appeared in magenta hue as the intermediate character between Ca-rich and K-rich feldspars. The combination of Na_2O and K_2O components is the index of igneous rock classification whether it is alkalic or not (Fig. 1). For example, the rock type showing high value of Na_2O+K_2O content is classified to the alkalic rock such as phonolite. If Na_2O+K_2O content is rich in the rock, the color shade on the image for it is expected to appear dark bluish hue. Consequently, the ASTER TIR range will represent a geological information that affects the alkaline components in the rock.

Phyllosilicate group are represented by chlorite, mica and serpentine. Biotite and muscovite in mica minerals are recognized in the silicic igneous rocks such as dacite and granite. The spectral curves tend to shift to longer wavelength range around 0.5 μm than the tectosilicate themselves.

Inosilicate group are represented by pyroxene and amphibole which are included typically in the intermediate igneous rocks. Fig. 5 (light) is shown for the reflectance curves of augite and hypersthene as examples of pyroxene group. The curve feature is representing broad shape ranging from band 11 to 14. These are indicating a similar pattern of the emissivity curves for basaltic trachy andesite and trachyte shown in Fig. 4. The intermediate igneous rock such as trachyte is usually abundant in pyroxene as a type of the mafic mineral. If it applies B:G:R=10:12:14 for the false color image, the color shade of the intermediate igneous rock should be appeared in magenta to purple hue.

Nesosilicate group are represented by olivine and garnet, which tend to be abundant in mafic and ulramafic igneous rocks. Usually, olivine is recognized as the phenocryst in basaltic rock and tends to become larger size in proportion to increase of alkaline component such as picrite (Na_2O+K_2O > 18%). The reflectance curves of olivine indicate the high reflectance and broad shape ranging from band 12 to 14 (Fig. 4). The emissivity curve of picrite has the absorption at same range. This behavior should be affected by olivine phenocryst in the rock. If it

Table 3. Band combinations and their expected advantages.

Band Combination	Expected Advantage
B:G:R=10:12:14	- Classification on the basis of tectosilicate whether the rock type is mafic or silicic.
	- Prediction of alkaline components of feldspar.
B:G:R=11:12:13	- Classification on the basis of alkaline content of the rock in the case of narrow range of SiO2 content

compares picrite with basalt at the point of emissivity behaviors, fine difference can be the maximum absorption range of picrite shifts to longer wavelength region than basalt. This considers affecting the nesosilicate mineral and also implying the behavior to representing the difference of total volume of alkaline content in the rock. At this point of view, if it applies B:G:R=11:12:13 for the false color image, the color shade of the alkaline rich rock such as picrite should be appeared in bluish. On the other hand, the poor alkaline rock such as basalt expects to appear greenish hue.

5. Analysis of ASTER TIR Data

First image of the Erta Ale range by the ASTER TIR was acquired in the nighttime on February 6, 2000, which was two months later after the launch of the satellite TERRA (Fig. 2). One year after, 4 more scenes were acquired anew and decorrelation stretch composite images of B:G:R=10:12:14 prepared to judge the constancy of the data quality (Fig. 3). The spectral information from the land surface keeps same condition except for the difference of color shade. A bright spot at the center of all images corresponds to the pit crater of the Erta Ale. This represents higher temperature condition than around surface because of the molten lava lake of the pit crater.

The volcanic rock type in the Erta Ale range is characterized by extensive compositional range from basalt to rhyolite. Basaltic rocks appear grayish white hue at the Alu Dala Filla area and the slope of the Erta Ale (Fig. 2). The large area of the slope at the Alu Dala Filla area is covered by flood or shield basalt. On the other hand, grayish white hue at the slope of the Erta Ale corresponds to the meandering basaltic lava flow from many fissures that occur in parallel to the main axis of the Erta Ale range. Magenta hue at the center of the Erta Ale corresponds to the recent viscous lava flow. There is no detail petrologic description on viscous lava flow in the number of past studies, but this considers that the rock type can classify to the intermediate composition such as basaltic trachy andesite or trachy andesite from the spectrum analysis (Fig. 4). Silicic lava with rich SiO_2 content appears light pink at western border of the Alu Horst and the center of the Borale Ale.

For more detail interpretation, we prepared the decorrelation stretch composite image and thermal logarithmic residual composite image (Fig. 6) and detail geological maps modified after F. Barberi, 1970 are shown in Fig. 7. We tried to classify the rock type with the ASTER TIR for the following subdivided three areas.

5.1 Alu-Dala Filla

This area is located at south of Lake Bakili and consists of lava fields surrounding the Alu volcanic horst and the Dala Filla small steep cone. This chain is mostly formed by fissural basaltic lava emitted on a large surface of very low slopes. At the SE of Lake Bakili, the submarine picritic basalt lava flows and the hyaloclastite rings are described as oldest outcrops in this area and the distribution of the old basalt is also found on the western side and in the middle at the Alu horst. Especially at the SE of Lake Bakili, the picritic lava flow appears dark bluish hue with the ring of pinkish hue in decorrelation stretch composite image. The spectral information for the picritic lava on the image is affected by band 11 spectral range in response to the low SiO_2 content and high alkaline content of the bulk rock composition. On the other hand, pinkish hue corresponding to the hyaloclastite ring is affected by band 13 range, because the hyaloclatite has the glassy matrix (amorphous silica). Fine color differences are recognized of the same basaltic lava field at the NE area of the Alu Horst. This might be affecting by the appearance of andesine phenocryst in the rock. Consequently, andesine rich basalt lava appears yellowish blue hue in response to the low emissivity at the band 11 range and on the contrary, andesine poor basalt appears more bluish hue in response to the high emissivity affecting olivine phenocryst in the rock. Comparing with these two types of lava, it is considered that andesine poor lava such as olivine basalt or picrite with high alkaline content (Na_2O+K_2O) is older eruption than andesine abundant lava. The Alu horst has ellipsoidal shape and elongated NNW-SSE is also built of old basaltic lava, which appears slightly darker bluish hue than peripheral lava field. This darker bluish hue also considers affecting the high alkaline content as same as SE of Lake Bakili. Accordingly, the geologic history on the eruption in this area represents the undifferentiation of magma clearly. Moreover, the Alu Horst itself appears more reddish hue than same horst structural range. This considers to be influenced by silica supply from later silicic volcanic activity of the NW side and the Dala Filla volcano. This silicic volcanic activity supports to the undifferentiation of magma in the eruption history. The Dala Filla volcano is formed by accumulation of rhyolitic lava flow extending

to the East. The lava constituting the sharp cone is the porphyritic rock with glassy matrix. Consequently, the silicic lava appears pinkish hue affecting rich SiO_2 content as the narrow area.

5.2 Borale Ale

According to the description by F. Barberi, 1970, the lava fields constituting the base of the Borale Ale unit have emitted through three different types of fissures. Lava activity at these fissures produced the median bulge-shaped shield volcano of the Eritorian direction. Large pahoehoe flows cover the whole summit. On the other hand, both side of the Borale Ale are covered by recent Aa lava flows. The central part of the Borale Ale is formed by the accumulation of viscous silicic lava flow that is characterized by the mainly blocky and the interbedded pyroclastics. Consequently, the silicic lava from the Borale Ale appears pink hue affecting rich silica content in response to band 13 spectral range. The recent Aa lava flows with spatter cones appear dark greenish hue. This considers affecting the feldspar in the rock. Same characteristics are recognized at the Ale Bagu. On the other hand, at the NW side of the Borale Ale volcano, trachyte volcanic activity are also determined by F. Barberi, 1970. Trachyte lava appears magenta hue in response to band 11 and 13 spectral range on the image. This is affected by intermediate rock composition between basalt and rhyolite. The appearance of pyroxene phenocryst or microphenocryst will be expected as the rock forming mineral. Light magenta hue is recognized at the peripheral slope of the Borale Ale up to the Erta Ale. This corresponds to the distribution of oldest lava flow in this area and the volcanic rock type will be expected as intermediate such as basaltic trachy andesite.

5.3 Erta Ale

The Erta Ale is presently the most active volcano of the whole Erta Ale range, in which it occupies a central position. It is mainly built by the accumulation of basaltic flow along median fissures of the volcanic chain. Basaltic lava flow appears yellowish blue hue with meandering feature at the slope. This should be affected by abundant andesine phenocryst in the rock. The top of the Erta Ale volcano is occupied by an elipsoidal caldera elongated NNW-SSE direction. The two pit-craters of the Erta Ale still contain molten lava lake. The oldest lava at the eastern side consist of picritic basalt, which was covered by subareal flows of plagioclase porphyritic and picritic basalts, which appear greenish blue or yellowish blue as same as the Alu-Dalafilla volcanic range. The recent lava flow fills the main part of the caldera and flows over its southern threshhold. The lava flow considers as the plagioclase porphyritic basaltic andesite, which appears pure magenta hue at the summit area and peripheral slope area with meandering feature.

As a conclusion, the following items are verified by the rock type classification in the Erta Ale range.

1). A usefulness to classify the volcanic rock types with the emissivity behavior based on the silicate minerals ranging from basalt to rhyolite by decorrelation stretch and logarithmic residual images of ASTER TIR.

2). A possibility of the influence of alkaline components to the spectral characteristics in addition to the SiO2 content in the rock on ASTER TIR image.

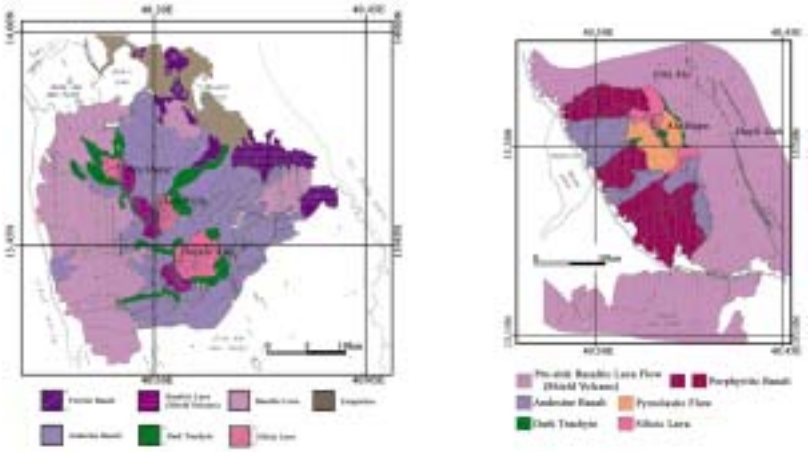

Fig. 7. Detail geological maps for the Alu - Dala Filla and Borale Ale <*left*> and the Erta Ale are< *right*> (modified after F. Barberi, 1970)

6. Discussion

6.1 Correlation with the SIR-C/X-SAR

The rock type classification with the ASTER TIR suggested the usefulness of the multi-spectral bands in thermal infrared region. We would like to discuss about the appropriation of our interpretation with the ASTER TIR with the SIR-C/X-SAR composite image of the Erta Ale Range co-registered in Fig. 2. The radar data is generally affected by the roughness of the surface. If the surface is smooth, the target object appears dark hue on the image, because the incidence wave behaves specular reflection as coherent component and then the signal to the antenna become weak or no return. On the other hand, in the case of coarse surface, incoherent component become increasing and signal to the antenna become strong and a result of this, the target object appear bright hue. This character of the radar sometimes applies for the geological interpretations. A SIR-C/X-SAR composite image of the Erta Ale range is showing bright and dark hued area. Bright hued area concentrates at the Alu Dala Filla to the Borale Ale and meandering feature can recognize at the peripheral slope of the Erta Ale. The distribution of them corresponds to the basalt from the result of our interpretation. Basaltic lava are characterized by two types of flows such as pahoehoe and aa. The former pahoehoe lava flow causes by the low viscosity due to the poor silica content and forms the smooth surface after cooling. On the contrary, the later aa lava flow is characterized by the rugged surface named for clinker. Consequently, it is considered that the aa lava flow shows bright hue affected by the roughness in the SIR-C/X-SAR composite image. This supports our interpretation with the ASTER TIR and insists the usefulness to classify the volcanic rock types by ASTER multi-spectral bands in thermal infrared region from 8.125 to 11.65 μm.

If brought up another influence to appear bright hue, it considers affecting the occurrence of many fissures which are parallel to NNW - SSW direction of the Erta Ale range. The most of the volcanic activities in the Erta Ale range are characterized by the eruption from fissures by geological point of view. These fissures might be affected to the SIR-C/X-SAR image. The bright hued area can also recognize of the silicic lava flow at the Dala Filla, Borale Ale and Ale Bagu. The Silicic lava has high viscosity, consequently, the lava dome and the high dense pyroclastic flow are observed as the typical volcanologic phenomena in its eruption process. The silicic lava dome usually shows rough surface such as the columnar jointed or blocky feature and the large volcanic breccias are composed of pyroclastics. Accordingly, these geological evidences consider as the cause of the bright hue in the Erta Ale range and are affected in the roughness on the SAR image.

6.2 Estimation of SiO_2 Content with ASTER TIR

ASTER has five spectral bands in thermal infrared range. Several preliminary studies to estimate SiO2 content by thermal infrared data (8.3-12.5 μm) were discussed by ERSDAC (1991, 1992) and MMAJ (1998-2000). Especially, MMAJ (2000) proposes the following equation for the SiO_2 estimation with band 10 to 13 of ASTER.

$$SiO_2\ (\%) = 56.20 - 271.09 \times \mathrm{Log}((Ems[10]+Ems[11]+Ems[12])/3/Ems[13]) \quad (1)$$

Ems[n] : emissivity of ASTER band n

We applied the above equation to estimate the SiO_2 content of volcanic rocks in the Erta Ale range. The methods of temperature - emissivity separation are suggested and discussed by various past papers. If it ignores the atmospheric correction, the emissivity values for each ASTER TIR bands can assume to be estimated by the log residual process. The effectivity of the log residual process for the geological application is introduced by S. Hook, 1992.

Fig. 8 shows the emissivity of the typical rock samples at the center wavelength of ASTER TIR and the relationship between the measured SiO_2 content in the laboratory and calculated SiO_2 content by the equation. The calculated SiO_2 content tend to estimate lower value than the measured content from minus 5 to 10 %, but the correlation suppose to be concordant on the whole.

Based on this result, we tried to estimate the SiO_2 content of the volcanic rocks ranging from magnesian transitional basalt to rhyolite in the Erta Ale range. The result almost corresponds with the actual geological feature and the spectral analysis of the ASTER TIR data (Fig. 9) in narrow range of the SiO_2 content. However, the estimated SiO_2 content for the silicic lava at Dala Filla, Borale Ale and Ale Bagu seem to be lower than the actual rock composition which was determined by past studies. Essentially, higher SiO_2 content should be estimated at these silicic lava fields than the Erta Ale center. This might represent an uncertainty of the equation for the SiO_2 estimation or real rock properties in the Erta Ale range. We need to take rock samples to compare with the measured SiO_2 content to validate the equation.

In addition to the result from Erta Ale range, we also applied for the ASTER TIR data to the Semail ophiolite (the Tethian oceanic lithosphere), which locates at the Arabian Peninsula (Fig. 10). The Semail ophiolite is composed of the mantle peridotite (the foliated orthopyroxene bearing harzburgite) in the lower unit to the basaltic andesite with hyaloclastite in the upper unit. The median unit is composed of the tonalite, diabase and gabbro. In petrological point of view, sequential rock compositions of Semail ophiolite are plotted at narrow range of SiO_2 content in contrast with the Erta Alle range. Profile line a-a' in Fig. 10 was set to cover from

the lower unit (a) to the upper unit (a'). The SiO_2 content increases gradually to the upper unit and implies a geological boundary in the ophiolite unit. This is also indicated on the logarithmic residual composite image as the appearance of magenta hue in the upper unit.

As a conclusion, the estimation of SiO_2 content with ASTER TIR is very useful for geological application and classifies the rock type of various rock types except for the accuracy of the equation.

6.3 Comparison with Daytime TIR Data

A daytime ASTER TIR data of Erta Ale range was acquired on June 28, 2000, which covers from Gada Ale to Borale Ale. We applied same method for the daytime data to discuss the effectiveness of the SiO2 estimation with ASTER TIR, because the temperature factor is superior to the emission factor in the daytime.

The logarithmic residual composite image and the SiO2 content map are shown in Fig. 11. Compared with Fig. 9, the false color hue on the logarithmic residual image of the daytime appears more clearly and enhanced feature rather than the nighttime data. It is able to distinguish between picritic and andesine basalts in Alu Dala Filla area. Picritic basalt appears blue and andesine basalt appears greenish yellow respectively. Differences of rock type also can recognize in the SiO2 content map. Picritic basalt appears less SiO_2 content (more bluish shade) than andesine basalt. The estimated SiO2 content with daytime and nighttime ASTER data indicate the concordant behavior in A-A' and B-B' traverse lines. However, relative changes of the SiO_2 content are affected to the content map of daytime TIR data. Consequently, it seems to be easy to distinguish between high and low SiO2 content area rather than the nighttime data in the same color scale. As a conclusion, the emission data in thermal infrared range in the daytime is also useful to classify the rock types same as the nighttime data. It tends to be enhanced rather than the nighttime data.

7. Conclusion

The ASTER TIR multi-spectral bands ranging from 8.125 to 11.65 μm are very useful to classify the rock type based on the emission spectrum affecting the SiO2 content. In addition to this result, we pointed out the influence of alkaline components of the rock to the emission spectrum. This might be affected by Si-O bond vibration caused by the atomic size of alkaline component inside SiO4 tetrahedral unit. However, we must investigate more detail about the influence of alkaline components to emission behavior.

The direct estimation of SiO_2 content with the emissivity from the ASTER TIR indicates concordant relation to the measured results in both nighttime and daytime data. Its result from the daytime implied more sensitive rather than nighttime and the other logarithmic residual composite image also indicated good relation to the actual rock type. Generally, the thermal factor is superior to the emission factor in the daytime, but we pointed out the usefulness to classify the rock type by the ASTER TIR multi-spectral bands in all the day.

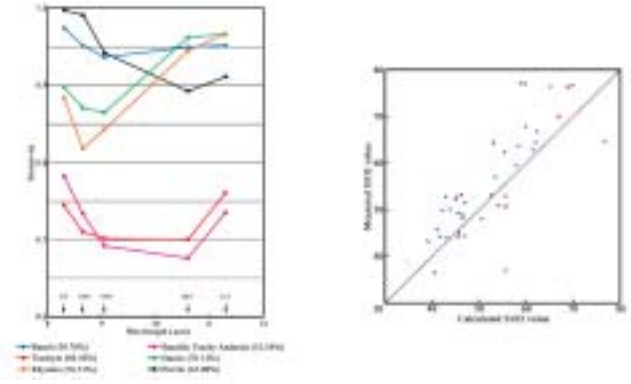

Fig. 8. Emissivity spectra of typical volcanic rock samples from laboratory measurement (left) and correlation between measured SiO2 content and calculated SiO2 content from the proposed equation by MMAJ (2000).

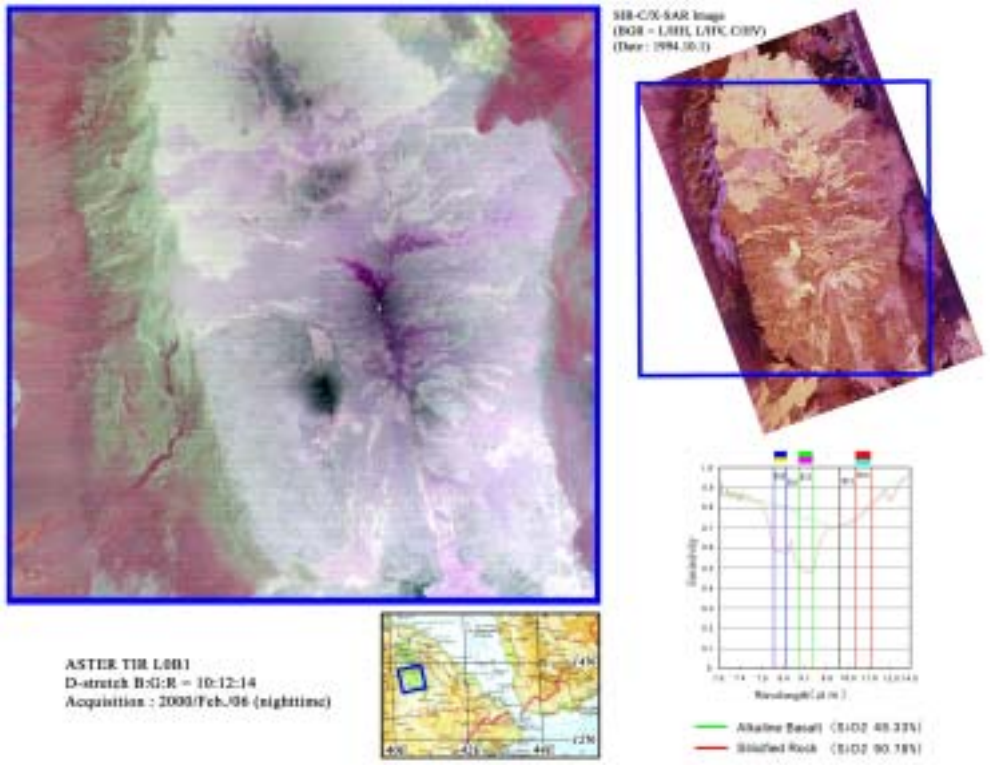

Fig. 2. ASTER TIR (thermal infrared radiometer) composite image of the Erta Ale range in the Afar Depression. ASTER TIR sensor is the first high spatial multi-spectral thermal infrared radiometer mounted on the satellite. A co-registered SIR-C/X-SAR Image Is covering the same area Is shown upper light (JPL/NASA).

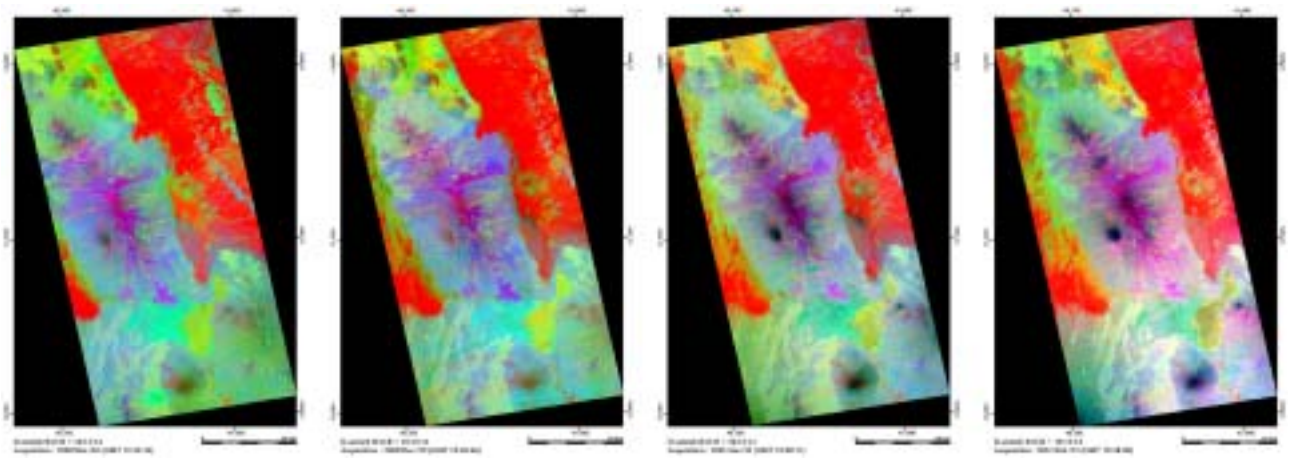

Fig. 3. Decorrelation composite images of the Erta Ale range in the nighttime. These 4 scenes were acquired anew on different date respectively after February 26, 2000.

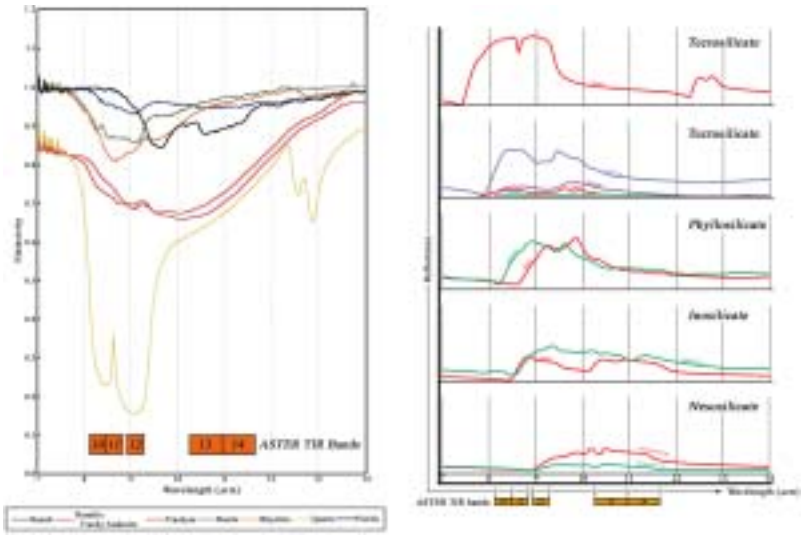

Fig. 4. The emissivity for various volcanic rocks ranging from picrite to rhyolite and massive quartz <*left*> (after Metal Mining Agency of Japan) and the reflectance for each silicate group <*right*> (after JPL/NASA).

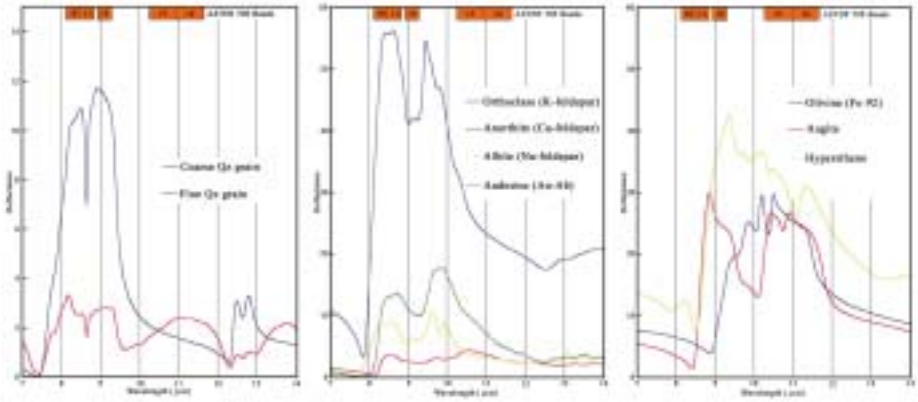

Fig. 5. The reflectance for typical silicate minerals, quartz <left>, feldspars <middle> and typical mafic minerals <right> (after JPL/NASA).

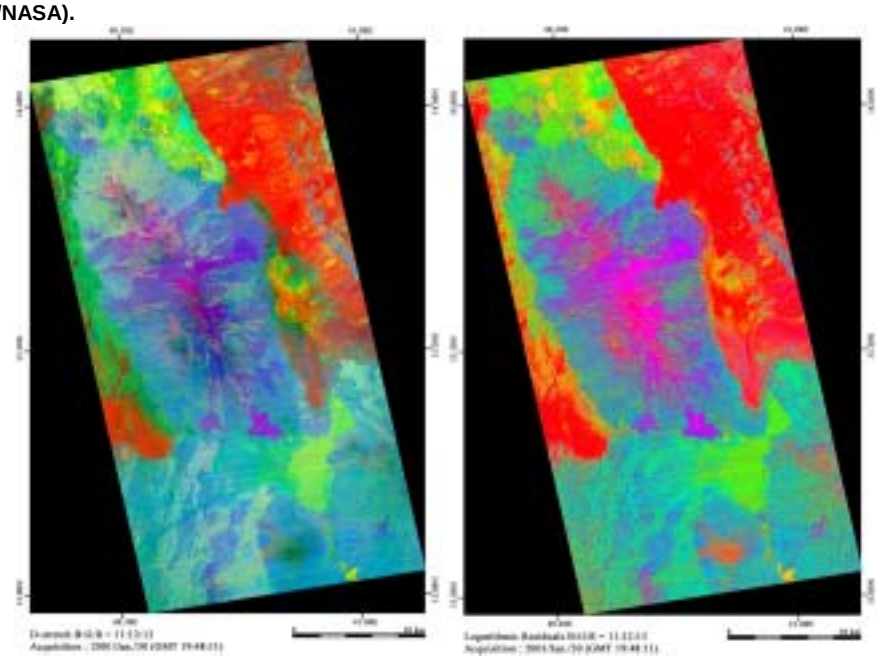

Fig. 6. Decorrelation stretch composite image <*left*> and logarithmic residual composite image <*right*> for the Erta Ale range.

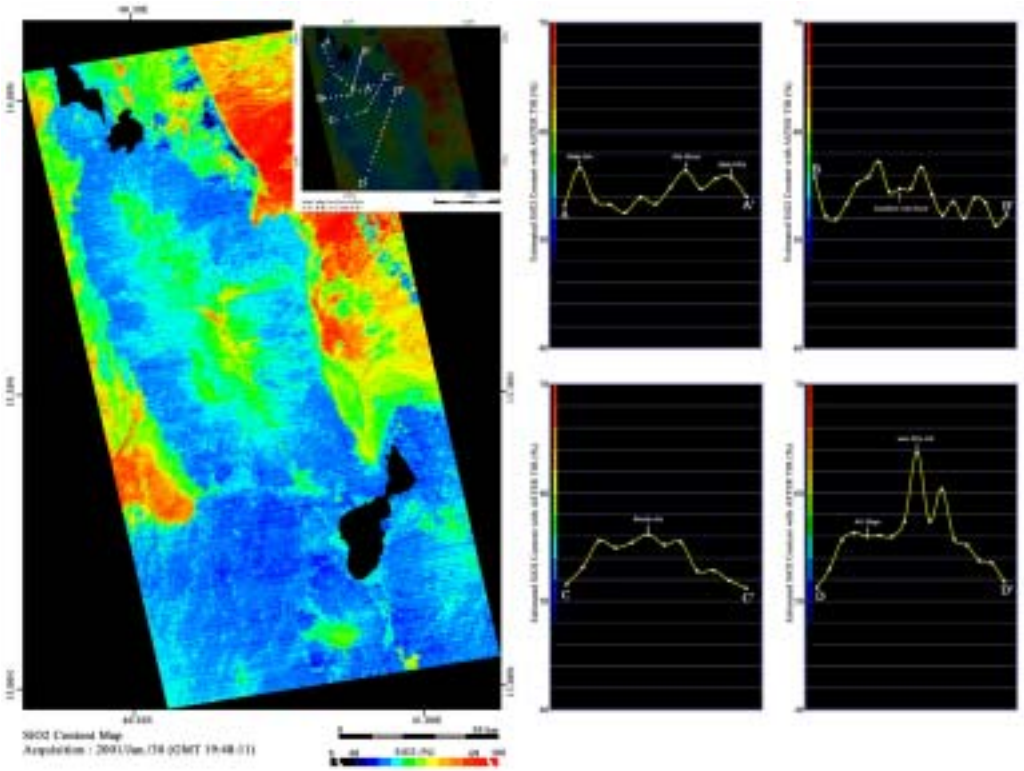

Fig. 9. SiO_2 content map for the Erta Ale range. A-A' to D-D' profiles are showing the detail of the lateral change of SiO_2 content in each traverse lines.

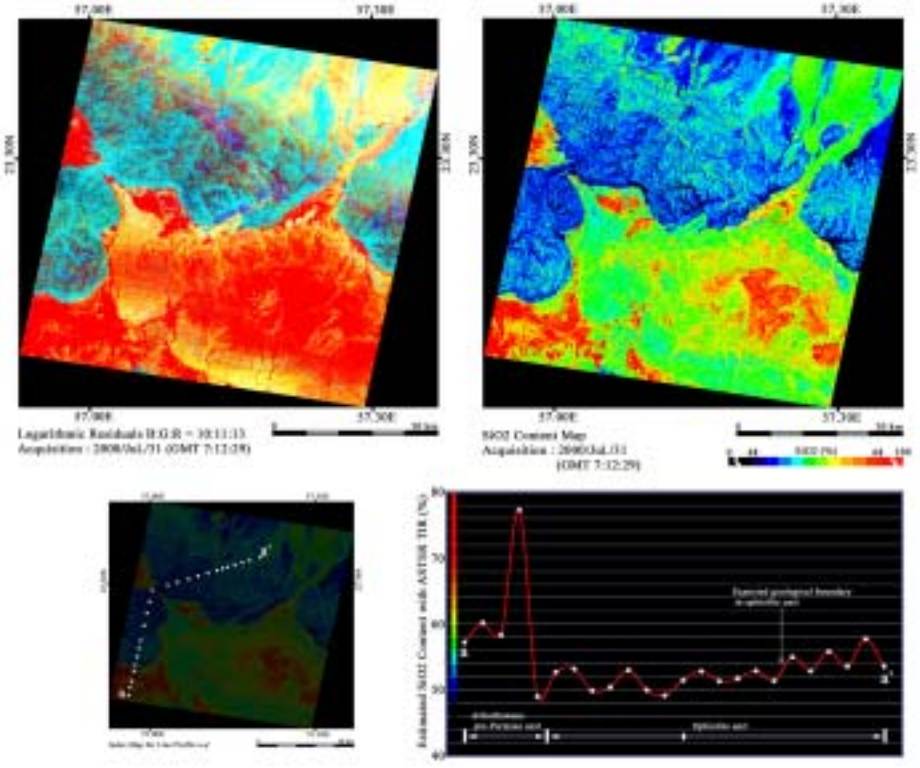

Fig. 10. Logarithmic residual composite image and SiO_2 map for the Semail Ophiolite, Oman. The detail profile of SiO_2 content on the a-a' traverse is shown lower right.

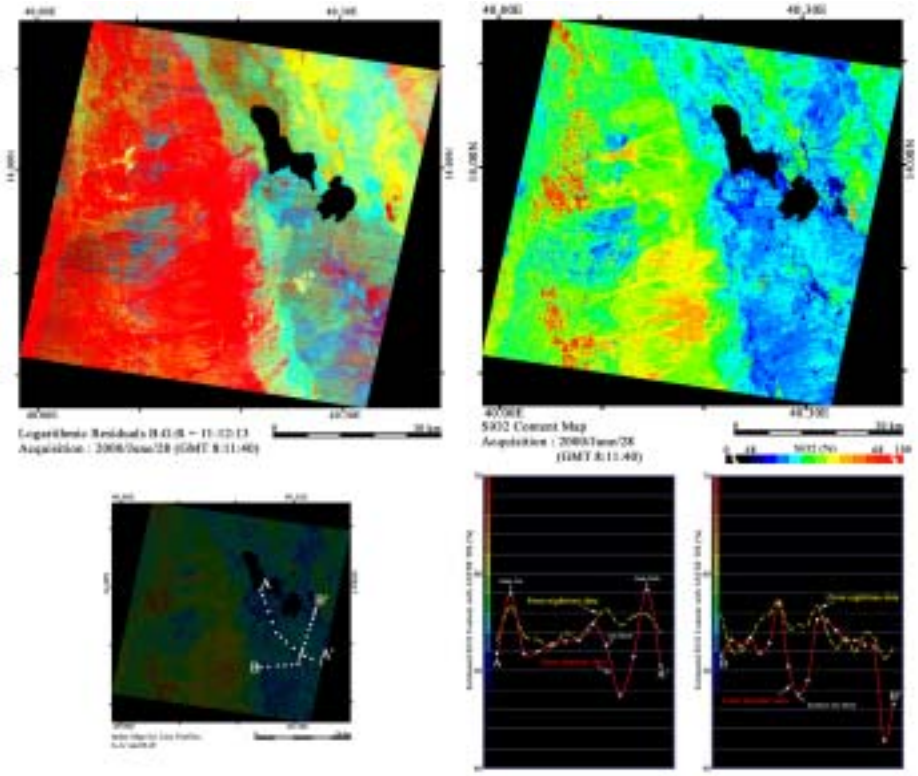

Fig. 11. Logarithmic residual composite image and SiO_2 map for the Erta Ale range by daytime data. The comparison with the estimated SiO_2 content between daytime and nighttime data are shown lower right.

8.References

1. F. Barberi and J. Varet,″The Erta Ale Volcanic Range (Danakil Depression, Northern Afar, Ethiopia)″, *Bull of Volcanol.*, 34, pp.848-917, 1970.
2. T. Chernet, W. K. Hart, J. L. Aronson and R. C. Walter, ″New age constrains on the timing of volcanism and tectonism in the northern Main Ethiopian Rift - southern Afar transition zone (Ethiopia)″, J. of volcanol. and geoth. res., 80, pp.267-180, 1998.
3. T. Korme, J. Chorowicz, B. Collet and F. F. Bonavia, ″Volcanic vents rooted on extension fractures and their geodynamic implications in the Ethiopian Rift″, J. of volcanol. and geoth. res., 79, pp.205-222, 1997.
4. R. George, N. Rogers and S. Kelley, ″Earliest magmatism in Ethiopia: Evidence for two mantle plumes in one flood basalt province″, Geology, 26, no.10, pp.923-926, 1998.
5. R. Pik, C. Deniel, C. Coulon, G. Yirgu, C. Hofman and D. Ayalew, ″The northwestern Ethiopian Plateau flood basalts: Classification and spatial distribution of magma types″, J. of volcanol. and geoth. res., 81, pp.91-111, 1998.
6. C. Oppenheimer and P. Francis, ″Implication of longeval lava lakes for geomorphological and plutonic processes at Erta Ale volcano, Afar″, J. of volcanol. and geoth. res., 80, pp.101-111, 1998.
7. G. Woldegabriel, J. L. Aronson and R. C. Walter, ″Geology, geochronology, and rift basin development in the central sector of the Main Ethiopia Rift″, Geo. Soc. of America Bull., 102, pp.439-458, 1990.
8. J. A. Barrat, S. Fourcade, B. M. Jahn, J. L. Cheminee and R. Capdevila, ″Isotope (Sr, Nd, Pb, O) and trace-element geochemistry of volcanics from the Erta Ale range (Ethiopia)″, J. of volcanol. and geoth. res., 80, pp.85-100, 1998.
9. P. A. Mohr, ″Regional Significance of Volcanic Geochemistry in the Afar Triple Junction, Ethiopia″, Geo. Soc. of America Bull., 83, pp.213-222, 1972.
10. S. J. Hook, A. R. Gabell, A. A. Green and P. S. Kealy, ″A comparison of techniques for extracting emissivity information from thermal infrared data for geologic studies″, Remote Sens. Environ., 42, pp.123-135, 1992.
11. Metal Mining Agency of Japan (MMAJ), ″Annual report, 2000″, 2000.